



OPEN Real time intravascular ultrasound evaluation and stent selection for cerebral venous sinus stenosis associated with idiopathic intracranial hypertension

Gang Luo^{1,2,3,4}, Raynald^{1,2,3,4}, Xu Tong^{1,2,3,4}, Yinuo Huang⁵, Zifei Han⁶, Dapeng Sun^{1,2,3,4}, Bo Wang^{1,2,3,4}, Baixue Jia^{1,2,3,4}, Zhenbo Shi^{1,2,3,4}, Feng Gao^{1,2,3,4}, Ning Ma^{1,2,3,4}, Zhongrong Miao^{1,2,3,4}✉ & Dapeng Mo^{1,2,3,4}✉

The value of intravascular ultrasound (IVUS) in the diagnosis and treatment of the venous system is not well established. Introducing a novel approach to utilizing IVUS to evaluate cerebral venous sinus (CVS) stenosis and select stent. Idiopathic intracranial hypertension (IIH) patients with CVS stenosis who underwent IVUS-guided stenting were included in the data analysis from January 2014 to February 2022. The degree of maximum stenosis was determined based on the cross-sectional area (CSA) measured by IVUS, and a stent selection method was applied in the study. Follow-up evaluations were conducted at 6 months to 1 year after endovascular treatment to assess symptom improvement. Additionally, repeated digital subtraction angiography (DSA) or Magnetic resonance venography (MRV) / CT venography (CTV) was performed to evaluate the stent patency at 6 months to 1 year post-procedure. The study included 61 patients. IVUS indicated a lower degree of stenosis compared to conventional DSA measurements when evaluating the degree of stenotic segments preprocedure ($74.84 \pm 10.12\%$ vs. $78.48 \pm 8.72\%$, $p = 0.035$). Post-procedural CSA of the most severe stenotic segments showed significant improvement ($36.44 \pm 8.07 \text{ mm}^2$ vs. $7.42 \pm 3.28 \text{ mm}^2$, $p < 0.001$). The stent achieved complete expansion (mean stent expansion index, 0.93 ± 0.20) with no significant change in the structure of the reference segment. The trans-stenotic mean pressure gradients (MPGs) across 61 patients significantly decreased from $11.00 \pm 6.23 \text{ mmHg}$ to $2.09 \pm 2.34 \text{ mmHg}$. 47 out of 61 patients received imaging follow-up; among them, 44 (93.6%) demonstrated stent patency in the follow-up imaging. IVUS has great potential to evaluate the degree and extent of CVS stenosis, assist stent selection, and optimize stent position during the interventional procedure in conjunction with DSA.

Keywords Cerebral venous sinus, Intravascular ultrasound, Digital Subtraction angiography

It was well recognized that cerebral venous sinus (CVS) stenosis is common among patients with Idiopathic Intracranial Hypertension (IIH),¹ and CVS stenting has increasingly become an effective treatment for these cases, particularly in refractory IIH cases^{2,3}.

The cross-section view of the CVS more closely corresponds to a triangular shape^{4–6}, which poses a difficulty in lesion assessment and appropriate stent selection using DSA. In addition to angiography, intravascular ultrasound (IVUS) can provide cross-sectional images of vessels and nearby structures, optimizing stent implantation. Recently, IVUS has been recommended for assessment of indeterminate coronary artery disease, carotid artery stenosis, or intracranial artery stenosis^{7–9}. However, the value of IVUS in the diagnosis and treatment of the venous system is not well established⁶.

¹Department of Interventional Neuroradiology, Beijing Tiantan Hospital, Capital Medical University, No.119 South 4th Ring West Road, Fengtai District, Beijing 100070, China. ²Beijing Key Laboratory of Translational Medicine for Cerebrovascular Disease, Beijing, China. ³China National Clinical Research Center for Neurological Diseases Center of Stroke, Beijing, China. ⁴Beijing Institute for Brain Disorders, Beijing, China. ⁵Department of Medicine, Beijing Fengtaiyouanmen Hospital, Beijing, China. ⁶University of International Business and Economics, Beijing, China. ✉email: zhongrongmiao@163.com; bjttmodp@163.com

The study aimed to assess the severity of CVS stenosis using real-time IVUS, and to propose a method for assisting stent selection based on IVUS.

Methods

Patients selection

Patients presenting with IIH symptoms and undergoing endovascular treatment (EVT) for CVS stenosis between January 1, 2014, and February 1, 2022, in our center were prospectively enrolled. IIH diagnosis was based on: (1) papilledema; (2) normal neurological examination, except for cranial nerve abnormalities; (3) neuroimaging revealing normal brain parenchyma without hydrocephalus, mass, or any structural lesion; (4) normal CSF (cerebrospinal fluid) composition; (5) elevated CSF opening pressure (greater than 250 mmH₂O); and (6) additional neuroimaging features supporting an IIH diagnosis. In addition, a diagnosis of IIH can be made even in the absence of papilledema if criteria 2 and 3 are satisfied for unilateral or bilateral abducens nerve palsy¹⁰. Candidates for VSS were selected based on intractable headaches, progressive papilledema, refractory to standard conservative treatment, and a diagnosis of CVS stenosis $\geq 50\%$ with trans-stenotic MPGs of at least 8 mmHg⁶. MRV, CTV, or DSA was used for screening and following up on CVS stenosis. Exclusion criteria included concurrent venous sinus thrombosis and poor-quality of images. A total of 272 patients were initially enrolled in the study. Of these cases, 85 cases underwent IVUS assessment, and 61 of them underwent IVUS-guided stent implantation (Fig. 1).

The study was approved by the institutional review boards of our hospitals, and informed consent was obtained pre-procedure.

DSA and IVUS assessment

DSA examination was necessary to confirm the diagnosis and assess the CVS stenosis before and after stent placement. IVUS was conducted with a 3.5 F, 20 MHz Eagle Eye IVUS probe transducer. The probe range was set to 20 mm for comprehensive visualization of the venous wall. DSA and IVUS images were assessed by two experienced readers who were blinded to the patient's clinical information. Any discrepancies were resolved by a third experienced reader.

In IVUS (Volcano Corporation, Rancho Cordova, CA, USA) assessment, the luminal lesion border was traced using a slow manual pullback technique at rates of approximately 1.0 mm/s, to calculate the luminal CSA. The reference segments in this study were defined as a segment 5 mm proximal and distal to the stenosis border and were confirmed as healthy segments without stenosis by IVUS. The method for calculating the degree of maximum stenosis of the lesion on IVUS is depicted in Fig. 2.

Three measurements were recorded: the luminal CSA of the site with the most severe stenosis (CSA 1), the luminal CSA of the distal reference segment (CSA 2), and the luminal CSA of proximal reference segment (CSA

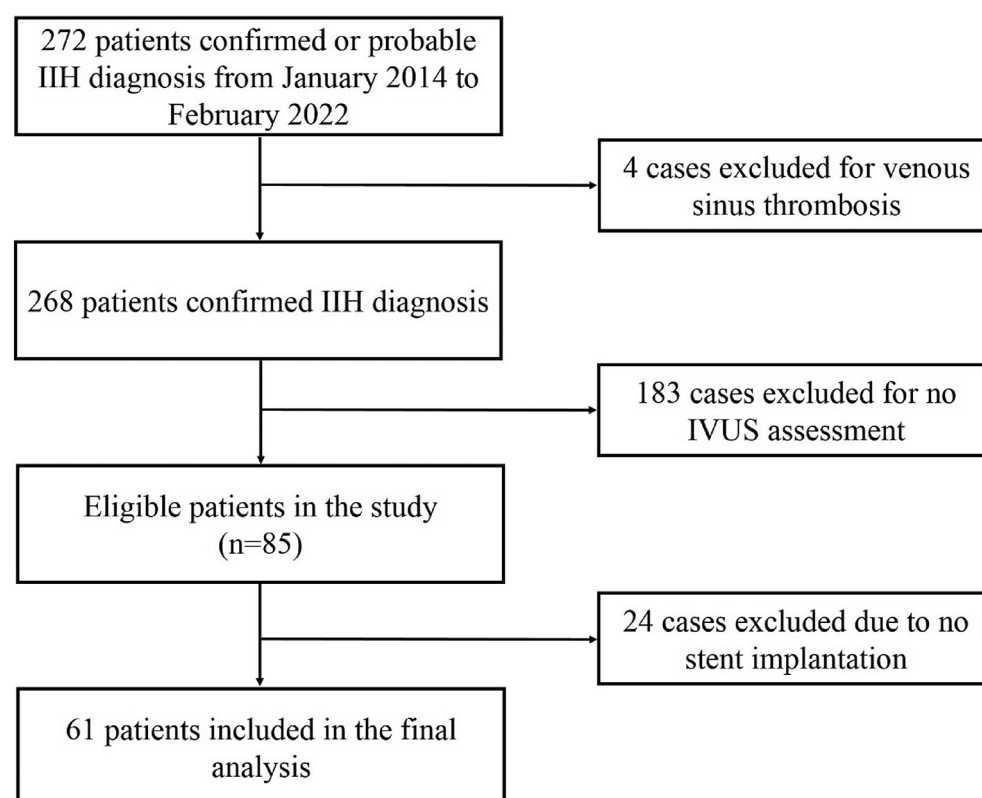


Fig. 1. Participants enrolled in the Intravascular Ultrasound guidance study on venous sinus stenting.

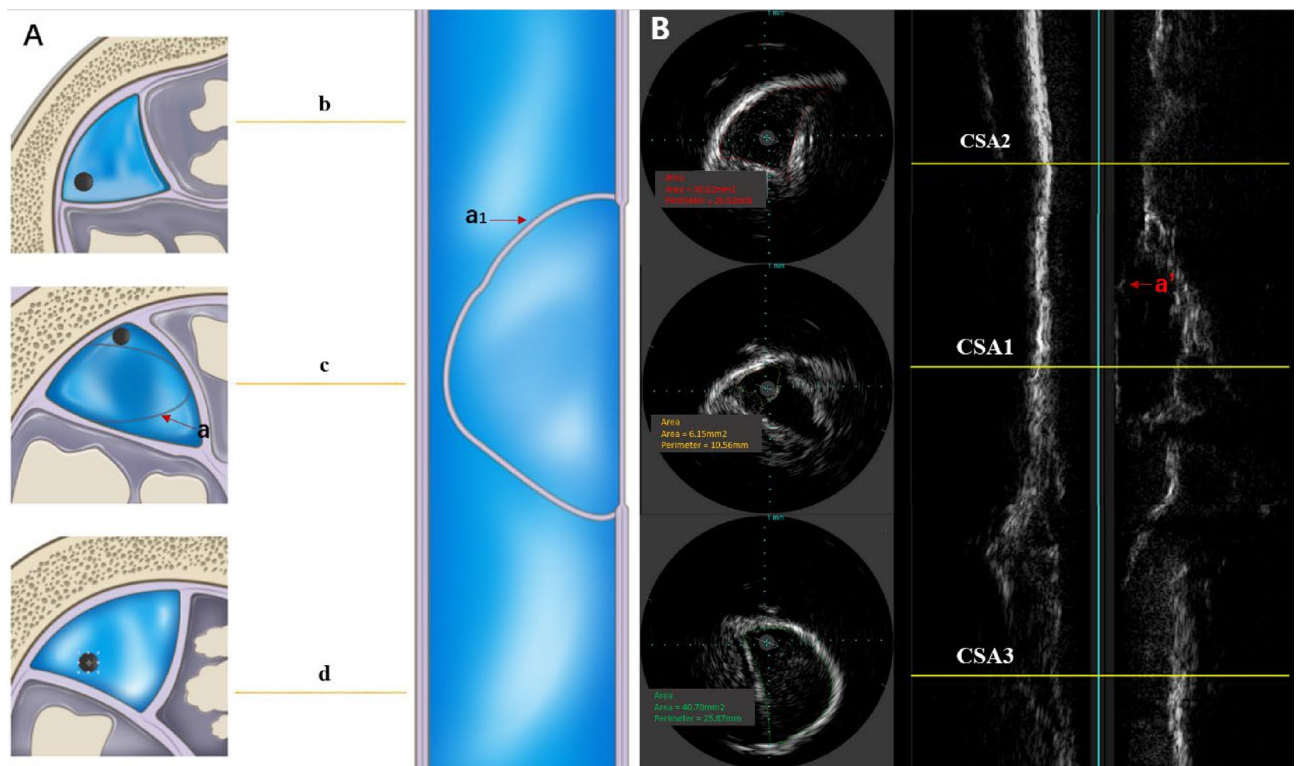


Fig. 2. A diagram presented CVS stenosis induced by arachnoid granulations, accompanied by IVUS images of the resulting stenosis. **(A)** The diagram displayed cross-sectional and longitudinal views of CVS stenosis sites caused by arachnoid granulations, along with reference sections from the proximal and distal segments. The blue section represented the CVS, while the black circles in the cross-sections marked the tips of the IVUS transducer. Sections b and d showed the cross-sectional and longitudinal views of the proximal and distal segments, respectively. Section c displayed the cross-sectional and longitudinal views of the stenosis sites caused by arachnoid granulations. Sections a and a1 exhibited significant arachnoid granulations within the CVS, leading to CVS stenosis. **(B)** IVUS images displayed cross-sectional and longitudinal views of CVS stenosis sites caused by arachnoid granulations. CSA₁ indicated the luminal CSA at the site of the most severe stenosis caused by arachnoid granulation, while CSA₂ and CSA₃ indicated the luminal CSA at the distal and proximal reference segments, respectively (a' depicted significant arachnoid granulation within the CVS, resulting in CVS stenosis). The Fig. 2A was generated by Adobe Illustrator CC 2022 (<http://www.adobe.com/cn/creativecloud/roc/business.html>).

3). The formula for the degree of stenosis is $(1 - [CSA_1 / (CSA_2 + CSA_3) / 2]) \times 100\%$. The length of CVS stenosis was defined as the distance between the distal and the proximal ends of the stenosis border.

Stenosis severity on DSA was determined using the method outlined by James et al.¹¹, the narrowest luminal diameter affected CVS, as well as the normal diameter of the CVS in the worst view on angiographic projection. Percent stenosis was calculated using the formula: $(1 - [\text{smallest diameter} / \text{normal diameter}]) \times 100\%$. The length of stenosis on DSA is calculated as the sum of the narrowest segment 1 (length between the distal stenosis border and maximum stenosis) and narrowest segment 2 (length between the proximal stenosis border and maximum stenosis). The formula of the length of stenosis on DSA is narrowest segment 1 + narrowest segment 2.

Stent selection

Considering that the CVS corresponds more closely to a triangular shape in cross-section view, the study introduced a novel stent selection method. The stent size and length were calculated using formulas derived from IVUS measurements of the proximal and distal reference segments of the lesion.

As illustrated in Fig. 3, R_2 represents the radius of circle A_2 , calculated using the formula: $\sqrt{A_2 / 2\pi}$. Here, A_2 refers to the average triangular area of the proximal (CSA₁) and distal (CSA₂) reference segments of the lesion.

R_3 denotes the radius of circle A_3 , derived from the formula: $\sqrt{A_2 / C_3}$. A_3 represents the inscribed circles of the lesion within the triangular structure of the CVS, as inferred from the proximal and distal reference segments. Additionally, C_3 is defined as the average perimeter of the triangular perimeter C1 and C2, representing the proximal and distal reference segments, respectively.

The stent diameter ($2R_1$) was determined to be within the range defined by $2R_2$ and $2R_3$, expressed mathematically as $2\sqrt{A_2 / 2\pi} \leq 2D_1 \leq 2\sqrt{A_2 / C_3}$ and $2(CSA_1 + CSA_2) / (C_1 + C_2) \leq 2D_1 \leq \sqrt{(CSA_1 + CSA_2) / 2\pi}$. The stent

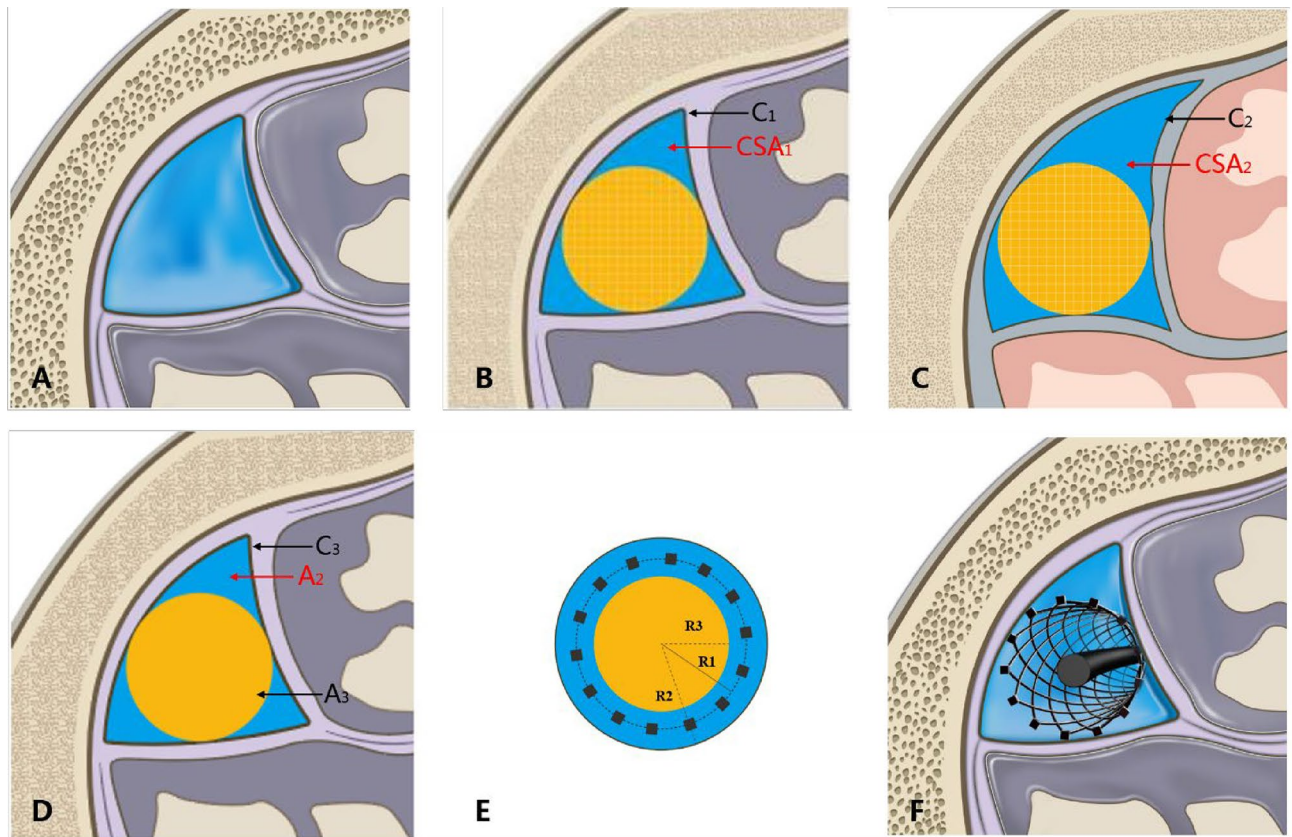


Fig. 3. Schematic illustration of the stent diameter selection based on IVUS measurement. (A) Cross-sectional illustration of venous sinuses and adjacent anatomical structures, the blue section indicated the CVS. (B) Cross-sectional illustration of proximal reference segment of the lesion. C_1 denoted the perimeter of triangle CVS in this segment, while CSA_1 represented its area. The yellow region indicated the area of the inscribed circles within the CVS triangle of the proximal reference segment. (C) Cross-sectional illustration of the distal reference segment of the lesion. C_2 denoted the perimeter of the CVS triangle in this segment and CSA_2 represented its area. The yellow region indicated the area of the inscribed circles within the CVS triangle of the distal reference segment. (D) Schematic illustration of the hypothesized lesion structure based on IVUS measurements of the proximal and distal reference segments. C_3 denoted the perimeter of the lesion's CVS triangle, derived from the IVUS measurements of C_1 and C_2 . A_2 represented the area of the lesion's CVS triangle, derived from CSA_1 and CSA_2 , while A_3 indicated the inscribed circles within this triangular structure, inferred from both reference segments. (E) Illustration of stent size selection for lesion, based on cross-sectional area and inscribed circles within the CVS triangular structure, derived from proximal and distal reference segments. The blue area represented the cross-sectional area of the CVS. The yellow area represented the area of inscribed circles within the CVS. The small black squares depicted the cross-sectional area of the stent. R_2 represented the radius calculated from the average cross-sectional area of proximal and distal reference segments of the CVS. R_3 was derived from the average area of inscribed circles within proximal and distal reference segments of the CVS. R_1 was the stent radius, which was between R_2 and R_3 . (F) Cross-sectional illustration of stent deployment in the CVS. The figure was generated by Adobe Illustrator CC 2022 (<http://www.adobe.com/cn/creativecloud/roc/business.html>).

length was determined by adding 10 mm to both sides of the distal and proximal stenosis borders, in addition to the length of the stenosis segment.

Self-expanding stents (Precise Carotid stent, Cordis, U.S.A; Wallstent, Boston Scientific, USA) with diameters ranging from 7.0 mm to 9.0 mm and lengths between 30 mm and 50 mm were utilized for stent implantation.

Stenting procedure

Before stenting, all patients received a daily dose of 75 mg clopidogrel and 100 mg aspirin for 3–5 days. Procedures were conducted under general anesthesia with intraoperative anticoagulation therapy (dosage 4000–6000 units) and intravenous heparin to maintain an activated clotting time above 250s¹². Prior to stenting, DSA was performed through arterial femoral access to assess stenosis features and select the worst view. IVUS evaluation and stenting followed a femoral transvenous approach using a short 8-Fr sheath. An 8-Fr guiding catheter was placed at the end of the internal jugular vein (IJV). A 6F intermediate catheter was advanced into the distal transverse sinus (TS) through the 8-Fr guiding catheter. The microcatheter (Rebar-27, Medtronic,

Minneapolis, MN) was used to access the superior sagittal sinus (SSS) under microwire guidance. Contrast agent was injected through the microcatheter into the SSS, TS, and sigmoid sinus (SigS). The transtenotic MPGs were measured by a microcatheter-attached pressure transducer, using a venographic roadmap with the worst projection angle of the stenosis and the mid-axillary line as the zero reference point. If the transtenotic MPGs of the CVS stenosis exceeded 8 mmHg, IVUS evaluation and stenting would be carried out. An IVUS probe transducer was advanced across the stenotic sinus segment over a microwire. The radiopaque IVUS transducer probe was slowly retracted from the distal reference segment point to the proximal reference segment point of the lesion using a slow manual pullback technique at rates of approximately 1 mm/Sec. 6. All IVUS images were displayed and recorded on a workstation. Following IVUS assessment the stenosis, balloon angioplasty predilatation was performed as the initial treatment. Predilatation was conducted at maximum of 6 atm for 60 s using a 5.0–6.0 mm balloon catheter (Sterling balloon catheter, Boston Scientific, U.S.A). Subsequently, stenting procedures were performed. The IVUS assessment was then repeated from the distal to proximal stenting site, yielding another recording. Post-stenting balloon dilatation was performed if the residual stenosis of the CSA exceeded 50% at the target lesion site, or if the transtenotic MPGs exceeded 8 mmHg post-stenting. The size of the post-stenting balloon was determined based on 0.8 times the target CVS reference diameter, ensuring adequate the stent stenosis coverage. Subsequently, IVUS and transtenotic MPGs were re-evaluated. The procedure ended when the residual stenosis of the CSA was less than 30% at the target lesion or when the transtenotic MPGs was less than 8 mmHg post dilatation.

Anticoagulation and antiplatelet

The patients were administered with low-molecular-weight heparin for 3 days post-procedure. They continued to take 100 mg of aspirin and 75 mg of clopidogrel daily for 3 months, followed by life-long use of aspirin or clopidogrel.

Follow-up protocol

Clinical assessments and radiographic examinations were performed 6 months to 1 year after stent placement. Restenosis was defined as stenosis exceeding 50% within the stent or at the edge of the stent, as verified by angiography.

Statistical analysis

Statistical analyses used SPSS Statistics version 21.0 (IBM SPSS, Armonk, NY, USA). Baseline and outcome data were presented as means (standard deviations) or medians (25th and 75th percentiles) for continuous variables and as frequencies or proportions for categorical variables. The paired-sample T test or nonparametric test (Wilcoxon test) was employed to compare mean differences. The categorical and binary data were compared between the groups using the χ^2 test or Fisher exact test, respectively. A p -value < 0.05 was considered statistically significant.

All methods were in accordance with the Declaration of Helsinki and approved by the Ethical Committee of Beijing Tiantan Hospital. All participants were fully informed of the nature of the study protocol and all gave their written consents regarding participation.

Results

Clinical characteristics of the patients before the procedure

Patients' baseline characteristics are reported in Table 1, with 52 out of the 61 patients (85.2%) being female. The mean body mass index (BMI) of the group was 27.8 ± 4.4 kg/m². The most common symptom was visual dysfunction, affecting 50 patients (82.0%). All patients exhibited increased CSF opening pressure, averaging 300.9 ± 46.1 cm H₂O. The findings also indicated that the primary lesion sites were frequently situated at the junction of the TS and SigS, impacting 45 patients (73.8%). Stenosis was most commonly found on the right side of the venous sinus, affecting 41 patients (67.2%).

IVUS and DSA for CVS stenosis assessment

Table 2 displays that the degree of maximum stenosis evaluated by DSA was more severe than that evaluated by IVUS before the procedure ($p = 0.035$), and milder than the IVUS assessment after the procedure ($p < 0.001$).

IVUS-guided stent implantation

A total of 74 stents were used in the 61 patients, with a single stent implanted in 50 cases and 24 stents in 11 cases due to long or tandem lesions. The stent sizes employed in this study were detailed in Table 3. The mean diameter of the stent was 7.94 ± 0.56 mm, with a mean length of 48.36 ± 11.76 mm across the 61 patients. IVUS-guided stent implantation was successful in all cases. A representative case of IVUS-guided CVS stenting is shown in Fig. 4.

According to the IVUS measurement results presented in Table 4, an appropriately sized and lengthened stent was selected for EVT. Two patients underwent post-stenting balloon dilatation due to the residual stenosis with a CSA exceeding 50% at the target lesion site. After stenting or post-stenting balloon dilatation, there was a significant improvement in the diameter and CSA of the most severely stenosed segments. The stents fully covered the stenotic segment ($p < 0.001$), and the CSA of the stenosis significantly improved post-procedure ($p < 0.001$), while the reference segment of the target lesion did not show significant change post-stenting ($p = 0.287$). The trans-stenotic MPGs across the 61 patients significantly decreased from 16.27 ± 8.71 mmHg pre-procedure to 1.30 ± 1.60 mmHg post-procedure.

Feature	Value
Gender, female	52 (85.2)
Age (mean \pm SD), y	36.8 \pm 10.2
BMI (mean \pm SD), kg/m ²	27.8 \pm 4.4
Hypertension	19 (31.1)
Dyslipidemia	2 (3.3)
Clinical duration	
Onset to EVT, median (IQR), months	4 (1, 12)
Aggravation to EVT, median (IQR), days	30 (30, 60)
Clinical presentation	
Headache	36 (59.0)
Tinnitus	12 (19.7)
Visual dysfunction	50 (82.0)
Binoculus	41 (67.2)
Ocellus	9 (14.8)
Vision acuity decline	42 (68.9)
Visual field defect	5 (8.2)
Dysmorphopsia	3 (4.9)
Amaurosis	7 (11.5)
Diplopia	5 (8.2)
Ophthalmic examination	
Papilledema	52 (85.2)
Vision acuity (mean \pm SD)	
Left	0.81 \pm 0.35
Right	0.81 \pm 0.37
Lumbar pressure, (mean \pm SD), mm H ₂ O	300.9 \pm 46.1
Location of stenosis, No. (%)	
Ts	12 (19.7)
Ts-SigS	45 (73.8)
Ts and SigS	2 (3.3)
Ts and Ts-SigS	1 (1.6)
SSS and Ts	1 (1.6)
Laterality of stenosis	
Lt, Rt nomal	1 (1.6)
Rt, Lt nomal	9 (14.8)
Bilateral	14 (23.0)
Lt, Rt hp or occlusion	5 (8.2)
Rt, Lt hp or occlusion	32 (52.2)

Table 1. Baseline characteristics. Data are expressed as No. (%) unless otherwise indicated. *BMI* body mass index, *IQR* interquartile range, *IVUS* intravascular ultrasound, *EVT* endovascular treatment, *TS* transverse sinus, *SigS* sigmoid sinus, *SSS* superior sagittal sinus, *Ts-SigS* junction of transverse sinus and sigmoid sinus, *hp* hypoplastic, *Lt* left, *Rt* right.

	Evaluated by IVUS	Evaluated by DSA	P Value
Base imaging data, (mean \pm SD)			
Rate of stenosis, (%)	74.84 \pm 10.12	78.48 \pm 8.72	0.035
Length of stenosis, mm	21.46 \pm 12.90	23.06 \pm 13.29	0.610
Degree of stenosis postprocedure, (mean \pm SD)	11.40 \pm 9.79	5.66 \pm 9.65	<0.001

Table 2. Angiographic and procedural characteristics for target lesions compared by IVUS and angiography. *TS* transverse sinus, *SigS* sigmoid sinus, *hp* hypoplastic, *Lt* left, *Rt* right, *IVUS* intravascular ultrasound, *DSA* digital subtraction angiography.

Stent	Diameter*, mm	Length†, mm	Number, n
Precise	8	30	25
	8	40	25
Wallstent	7	50	14
	9	50	10
Mean, (mean ± SD)	7.94 ± 0.56	48.36 ± 11.76	

Table 3. Summary of the stent sizes utilized in the study. * The diameter of the 74 stents. † The lengths of the 74 stents from 61 patients were recorded.

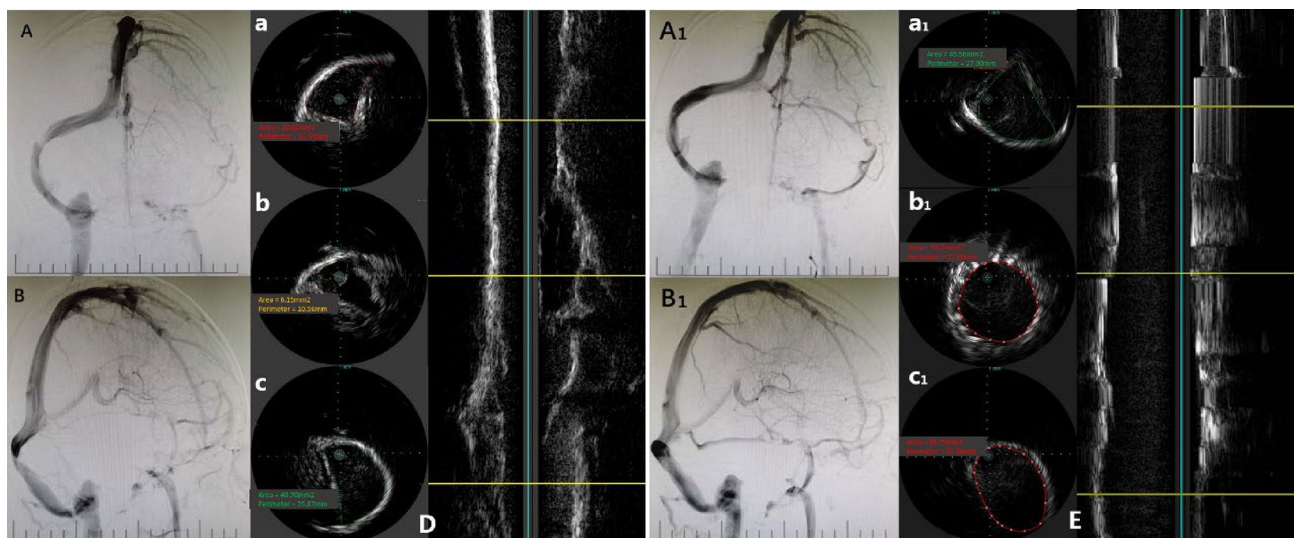


Fig. 4. The patient presented with a headache and persistent deterioration of visual function, despite medical treatment for 8 months. **A** and **B**: The angiogram with venous phase images shows severe stenosis of the right transverse sinus before stenting from both the anterior-posterior and oblique views, the transtenotic mean pressure gradient was 14mmHg. Note that there is stenosis of both transverse sinuses. **A₁** and **B₁**: Angiogram with venous phase images demonstrating right transverse sinus post stenting from anterior-posterior view and oblique view. Note obvious change in flow dynamics with 2mmHg of transtenotic mean pressure gradient. **D**: Intravascular ultrasound (IVUS) demonstrating echogenic material with a significantly decreased diameter of the right transverse sinus. **(a)** distal reference segment of tight stenosis on IVUS. **(b)** tight stenosis on IVUS. **(c)** proximal reference segment of tight stenosis on IVUS. **E**. **a₁**, distal reference segment on IVUS post-stenting. **b₁**, IVUS post-stent deployment demonstrated increased cross-sectional area (CSA) at the narrowest site of the right transverse sinus prior to stenting. **c₁**, proximal reference segment on IVUS post-stenting.

Follow-up outcomes

Clinical information follow-ups were completed for all patients (Table 5). Repeat radiological studies were performed in 47 out of 61 (77.0%) patients. Among the patients who had headaches as a symptom, 91.7% showed improvement or disappearance of their symptoms. The visual function did not significantly change for 5 patients, besides 2 patients experienced worsened symptoms. All 5 patients had a prolonged history of symptoms, and ophthalmoscopic examination revealed severe optic atrophy before the procedure.

Discussion

The cross-section view of the CVS more closely corresponds to a triangular shape^{4–6}, which poses difficulty in lesion assessment and appropriate stent selection. Boddu et al. measured the diameter of CVS stenosis by using IVUS and DSA. The results suggested that the degree of stenosis observed on DSA was significantly higher than that on IVUS¹³. Boddu SR et al. used MRV and IVUS to evaluate the baseline CVS. Compared with IVUS measurements, three-dimensional contrast enhancement MRV overestimated the measurements of dimensions, including maximum diameter, area, and perimeter⁵. Although IVUS was used to assess the lesion and guide stent implantation, none of the studies addressed how to select an appropriate stent. Therefore, in our patient cohort, we introduced a method for stenosis evaluation and stent selection using IVUS. In our study, we found that calculating the degree of stenosis for the triangular structure of CVS using CSA and perimeter measurements obtained by IVUS may be more reasonable. As shown in Table 2, the degree of the maximal stenosis measured by DSA was higher preprocedure and lower postprocedure than that measured by IVUS, indicating potential overestimate or underestimate by DSA compared with IVUS measurements. While there were no significant

Variability	Preprocedure		Postprocedure		P value
	Mean		Mean		
	Distal	Proximal	Distal	Proximal	
CSA of reference segment, mm ² , (mean ± SD)	38.24 ± 6.97		39.55 ± 6.56		0.287
	36.40 ± 8.33	40.07 ± 8.47	37.79 ± 8.02	41.31 ± 8.47	
Perimeter of reference segment, mm, (mean ± SD)	25.42 ± 2.46		24.92 ± 2.57		0.273
	24.67 ± 3.01	26.18 ± 2.73	24.45 ± 3.08	25.39 ± 2.57	
D derived from A1 and A2, mm, (mean ± SD) D1 D2	7.95 ± 0.65	5.99 ± 0.81	7.94 ± 0.60*		NA
CSA of stenosis, mm ² (mean ± SD)	7.42 ± 3.28		36.44 ± 8.07		< 0.001
Length of stenosis or stent, mm, (mean ± SD)	21.46 ± 12.90		48.36 ± 11.76		< 0.001
Stent expansion index	NA		0.93 ± 0.20		NA
MPG, mmHg	16.27 ± 8.71		1.30 ± 1.60		< 0.001
MDP	23.96 ± 4.71		12.25 ± 5.25		
MPP	9.70 ± 3.28		10.93 ± 4.61		

Table 4. Target lesion characteristics pre-postprocedure guided by IVUS. CSA cross-sectional area, MPG mean pressure gradient, MDP mean distal pressure, MPP mean proximal pressure, A₁ a circle area equal to the average value area of reference segment, A₂ a inscribed circle area of reference segment, D diameter, D₁ diameter derived from A₁, D₂ diameter derived from A₁, * mean diameter derived from minimum diameter and maximum diameter passing through the center of the most severe stenosis.

Follow up items	6 months to 1 year after treatment
Radiologic follow-up, n(%)	47 (77.0)
DSA	42 (68.9)
CTV/MRV	5 (8.2)
In-stent restenosis	2 (4.3)
Dural arteriovenous fistula	1 (2.1)
Clinical follow-up	
Headache (n = 36)	
Unchanged or worsened	3 (8.3)
Improved	4 (11.1)
Disappeared	29 (80.6)
Tinnitus (n = 12)	
Unchanged or worsened	2 (16.7)
Improved	1 (8.3)
Disappeared	9 (75.0)
Papilledema (n = 52)	
Unchanged or worsened	3 (5.8)
Improved	11 (21.2)
Normal	38 (73.0)
Vision dysfunction (n = 50)	
Unchanged or worsened	7 (14.0)
Improved	11 (22.0)
Normal	32 (64.0)

Table 5. Outcome after IVUS-Guided dural venous sinus stenting. IVUS intravascular ultrasound, DSA digital subtraction angiography, CTV CT venography, MRV magnetic resonance venography. Data are expressed as No. (%).

differences in stenosis length between DSA and IVUS measurements, DSA may overestimate the lesion length compared with IVUS measurements. These findings support previous studies¹³.

For stent implantation in patients with CVS stenosis, using an oversized stent may not only significantly alter the original triangular contour of the CVS, but also impede the outflow of cortical veins as they enter the CVS, resulting in life-threatening complications such as hemorrhage, venous infarction, and seizures^{14,15}. Conversely, an undersized stent may increase the risk of restenosis. Therefore, selecting the appropriate stent size and length can prevent in-stent stenosis and reduce the duration of medical treatment^{16,17}. In our study, we employed a new method to select the stent using IVUS. With this method, the mean stent size was 7.94 ± 0.56 mm, which fell between the diameter of the circle with an area equal to the average area of the reference segments

(7.95 ± 0.65 mm) and the average diameter of an inscribed circle within the CVS, plus the average triangle perimeter of the reference segments (5.99 ± 0.81 mm). The mean stent expansion index was 0.93 ± 0.20 . Our data demonstrated that the stent achieved complete expansion (expansion index > 0.8) per IVUS assessment criteria for coronary artery stent implantation¹⁸. Additionally, the transtenotic MPGs of all patients significantly decreased after the procedure, showing promising results.

Despite most of the patients reporting significant improvement in their symptoms during the follow-up, three patients complained of aggravated headaches, two of whom had poor visual function and exacerbated tinnitus. A follow-up DSA revealed that one patient developed a dural arteriovenous fistula (DAVF), the symptom was largely improved after DAVF embolization. The other two patients experienced stent restenosis. One patient presented tandem lesions, and a stent was implanted for each lesion, resulting in a total of two stents. Repeat imaging suggested that the restenosis was located at the edge of the stent between the two. For another patient with in-stent stenosis, the lesion was too extensive to be adequately covered by one stent, so two stents were implanted. Radiological follow-up detected that the stent had separated from its former overlapped site, and restenosis occurred at this site. However, the symptoms of two patients were resolved after a third stent was implanted at the stenotic site. The in-stent restenosis at the stent edge of was probably caused by negative remodeling or intimal hyperplasia¹⁹. Conversely, using a tandem stent may lead to subacute thrombosis development²⁰. Regarding the patients whose visual function did not significantly change after the stenting, all of them had a long history of symptoms, and ophthalmoscopic examination revealed severe optic atrophy before the procedure, which was difficult to reverse²¹.

Limitations

The small sample size and our single center of IIH patients with CVS restricted our study. Further large-scale studies are needed to validate our evaluation method for CVS stenosis and stent selection using IVUS. Additionally, the stents utilized in the procedure are not tailored for CVS stenosis. The future development of dedicated devices for CVS stenosis will hopefully overcome this limitation.

Conclusions

IVUS possesses potential to assess the severity and extent of CVS stenosis, aid in stent selection, and optimize stent position during the interventional procedures when used alongside DSA.

Data availability

The data used in this study can be available upon reasonable request from the corresponding Author.

Received: 7 October 2024; Accepted: 29 April 2025

Published online: 11 May 2025

References

- Satti, S. R., Leishangthem, L. & Chaudry, M. I. Meta-analysis of Csf diversion procedures and dural venous sinus stenting in the setting of medically refractory idiopathic intracranial hypertension. *AJNR Am. J. Neuroradiol.* **36**, 1899–1904 (2015).
- Kanagalingam, S. & Subramanian, P. S. Cerebral venous sinus stenting for pseudotumor cerebri: A review. *Saudi J. Ophthalmology: Official J. Saudi Ophthalmological Soc.* **29**, 3–8 (2015).
- Fargen, K. M. et al. Recommendations for the selection and treatment of patients with idiopathic intracranial hypertension for venous sinus stenting. *J. Neurointerv Surg.* **10**, 1203–1208 (2018).
- Lublinsky, S. et al. Automated cross-sectional measurement method of intracranial dural venous sinuses. *AJNR Am. J. Neuroradiol.* **37**, 468–474 (2016).
- Boddu, S. R., Gobin, P., Oliveira, C., Dinkin, M. & Patsalides, A. Anatomic measurements of cerebral venous sinuses in idiopathic intracranial hypertension patients. *PloS One.* **13**, e0196275 (2018).
- Raynald, Chen, N. et al. Intravascular ultrasound characteristics of different types of stenosis in idiopathic intracranial hypertension with venous sinus stenosis. *J. Neurointerventional Surg.* **16**, 506–511 (2024).
- Levine, G. N. et al. 2011 Accf/aha/scai guideline for percutaneous coronary intervention. A report of the American college of cardiology foundation/american heart association task force on practice guidelines and the society for cardiovascular angiography and interventions. *J. Am. Coll. Cardiol.* **58**, e44–122 (2011).
- Clark, D. J., Lessio, S., O'Donoghue, M., Schainfeld, R. & Rosenfield, K. Safety and utility of intravascular ultrasound-guided carotid artery stenting. *Catheterization Cardiovasc. Interventions: Official J. Soc. Cardiac Angiography Interventions.* **63**, 355–362 (2004).
- Joan, M. M. et al. Utility of intravascular ultrasound examination during carotid stenting. *Ann. Vasc. Surg.* **23**, 606–611 (2009).
- Raynald, Huo, X. et al. Characteristics and outcomes of the idiopathic intracranial hypertension treatment in intrinsic and extrinsic stenosis: A single-center experience in China. *Neurol. Therapy.* **10**, 1029–1044 (2021).
- West, J. L. et al. Correlation between angiographic stenosis and physiologic venous sinus outflow obstruction in idiopathic intracranial hypertension. *J. Neurointerv Surg.* **11**, 90–94 (2019).
- Asif, H. et al. Idiopathic intracranial hypertension: 120-day clinical, radiological, and manometric outcomes after stent insertion into the dural venous sinus. *J. Neurosurg.* **129**, 723–731 (2018).
- Boddu, S. D. M. & Patsalides, A. Role of intravascular ultrasound in the intracranial cerebral venous sinus angioplasty and stenting. *J. Neurointerv Surg.* **7**(Suppl 1), A92–A93 (2015).
- Raper, D. M. S. et al. Patency of the vein of Labbe after venous stenting of the transverse and sigmoid sinuses. *J. Neurointerv Surg.* **9**, 587–590 (2017).
- Dinkin, M. J. & Patsalides, A. Venous sinus stenting for idiopathic intracranial hypertension: where are we now? *Neurol. Clin.* **35**, 59–81 (2017).
- Lenck, S. et al. Stenting of the lateral sinus in idiopathic intracranial hypertension according to the type of stenosis. *Neurosurgery* **80**, 393–400 (2017).
- Shazly, T. A. et al. Venous sinus stenting shortens the duration of medical therapy for increased intracranial pressure secondary to venous sinus stenosis. *J. Neurointerv Surg.* **10**, 310–314 (2018).
- Sonoda, S. et al. Current clinical use of intravascular ultrasound imaging to guide percutaneous coronary interventions. *Cardiovasc. Intervention Ther.* **35**, 30–36 (2020).

19. Ichimoto, E. et al. Mechanism of edge restenosis after sirolimus-eluting stent implantation. *J. Invasive Cardiol.* **24**, 55–57 (2012).
20. Sun, X. et al. Risk factors of subacute thrombosis after intracranial stenting for symptomatic intracranial arterial stenosis. *Stroke* **48**, 784–786 (2017).
21. Attia, R. et al. Risk factors associated with progression from papilloedema to optic atrophy: results from a cohort of 113 patients. *BMJ Open. Ophthalmol.* **8** (2023).

Acknowledgements

The Study Funded by Beijing Municipal Science & Technology Commission (Z221100007422053) and the Beijing Municipal Administration of Hospitals Incubating Program (PX2017009) to Dapeng Mo and Youth Training Program of Beijing Hospitals Authority (No. QML20190505) to Gang Luo.

Author contributions

Gang Luo: drafted the manuscript; Raynald -, Xu Tong, Dapeng Sun: critical revision of manuscript for intellectual content; Yinuo Huang, Zifei Han, Bo Wang, Baixue Jia, Zhenbo Shi.: performed the data collection and data analysis; Feng Gao, Ning Ma: study supervision; Zhongrong Miao and Dapeng Mo: study concept and design, analysis and interpretation of data, critical revision of manuscript for intellectual content.

Declarations

Competing interests

The authors declare no competing interests.

Additional information

Correspondence and requests for materials should be addressed to Z.M. or D.M.

Reprints and permissions information is available at www.nature.com/reprints.

Publisher's note Springer Nature remains neutral with regard to jurisdictional claims in published maps and institutional affiliations.

Open Access This article is licensed under a Creative Commons Attribution-NonCommercial-NoDerivatives 4.0 International License, which permits any non-commercial use, sharing, distribution and reproduction in any medium or format, as long as you give appropriate credit to the original author(s) and the source, provide a link to the Creative Commons licence, and indicate if you modified the licensed material. You do not have permission under this licence to share adapted material derived from this article or parts of it. The images or other third party material in this article are included in the article's Creative Commons licence, unless indicated otherwise in a credit line to the material. If material is not included in the article's Creative Commons licence and your intended use is not permitted by statutory regulation or exceeds the permitted use, you will need to obtain permission directly from the copyright holder. To view a copy of this licence, visit <http://creativecommons.org/licenses/by-nc-nd/4.0/>.

© The Author(s) 2025